

Equine diagnostic developments

Author : Annamaria Nagy, Sue Dyson

Categories : [Equine](#), [Vets](#)

Date : January 16, 2017

Diagnostic imaging is an integral part of most veterinary investigations. This article focuses on advances in equine diagnostic imaging that have expanded our knowledge in the field of equine orthopaedics.

A summary is provided of clinically relevant articles published in the past 12 months that have enhanced our knowledge of normal anatomical variations or pathological conditions.

Neck

Several papers focused on anatomical variations in the caudal aspect of the cervical spine, with most attention given to the ventral process of the 6th cervical vertebra (C6).

The ventral process is a large ventral expansion of the caudal part of the transverse process, officially named “ventral lamina” in *Nomina Anatomica Veterinaria*. The ventral process is bilaterally present on the left and right transverse processes and anomalies can be seen either unilaterally or bilaterally. A prevalence for anomalies of 18.7% has been previously documented in a small Australian study with overrepresentation in Thoroughbreds (May-Davis, 2014).

Santinelli et al (2016) evaluated anatomical variations of the spinous and transverse processes in the caudal cervical vertebrae and the first thoracic vertebra (T1) in 270 horses. Horses that had undergone cervical radiography were included and no clinical information on the horses was available.

The spinous process of the 7th cervical vertebra (C7) was identified in 76.1% of horses (**Figures 1 and 2**) and included three variant shapes – sharp triangular, rounded triangular and spur-like. The spinous process of the T1 was present in 76.9% of horses and was either high and pronounced (73.2%; **Figures 2 and 3**) or short and squat (26.8%; **Figure 1**). The ventral process of the C6 was transposed on to the ventral aspect of the C7 in 13.3% of horses (**Figure 1**), either unilaterally or bilaterally. A small separate centre of ossification was present at the caudal aspect of the ventral process of C6 in 4.8% of horses.

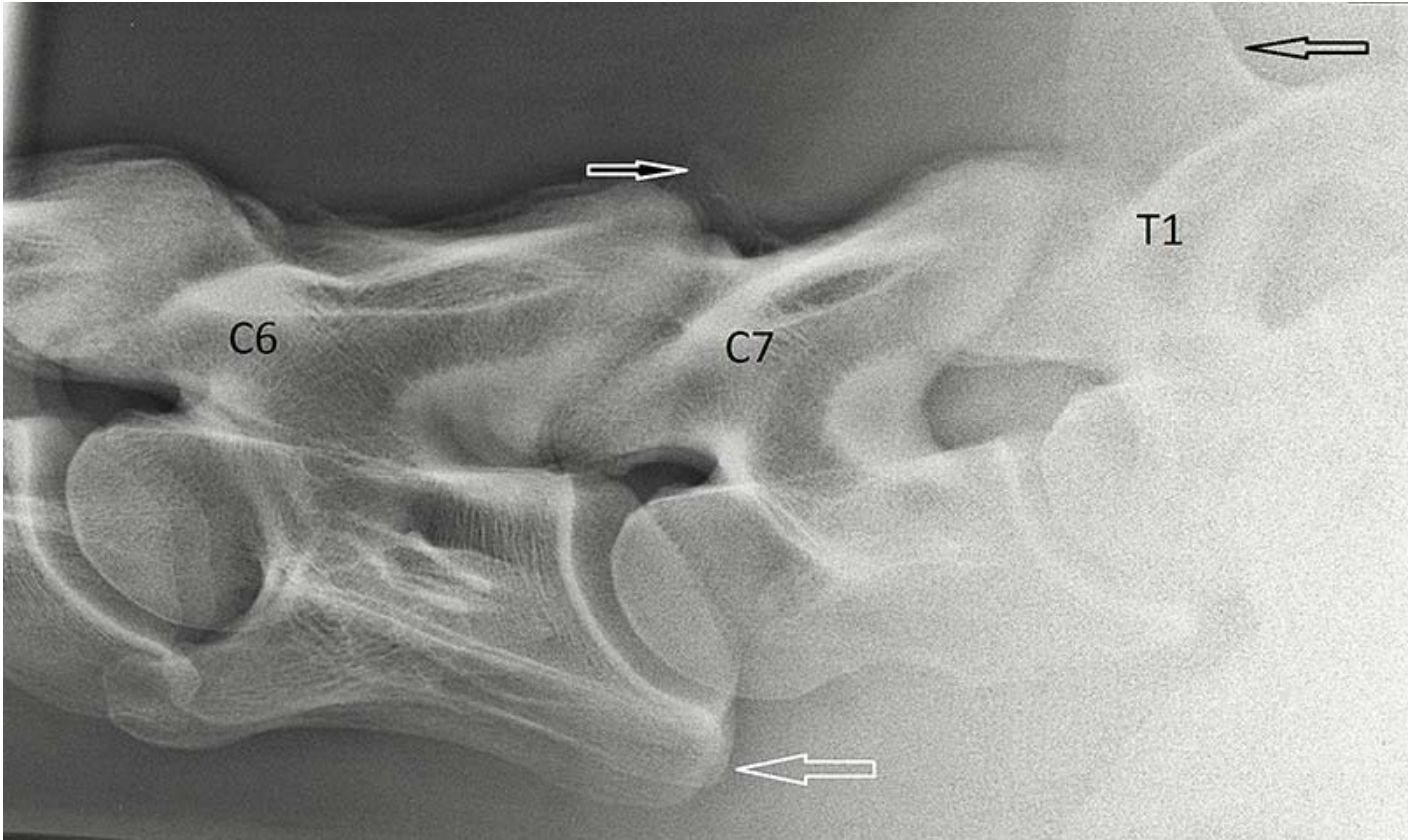


Figure 1. Lateral-lateral radiograph of the 6th and 7th cervical (C6 and C7) and 1st thoracic (T1) vertebrae. There is a small, but well-defined, triangular-shaped spinous process on C7 (black and white arrow). The spinous process of T1 is tall and pronounced (black arrow; its proximal aspect is not included in the image). The ventral processes are located on C6 (white arrow), indicating no anomaly.

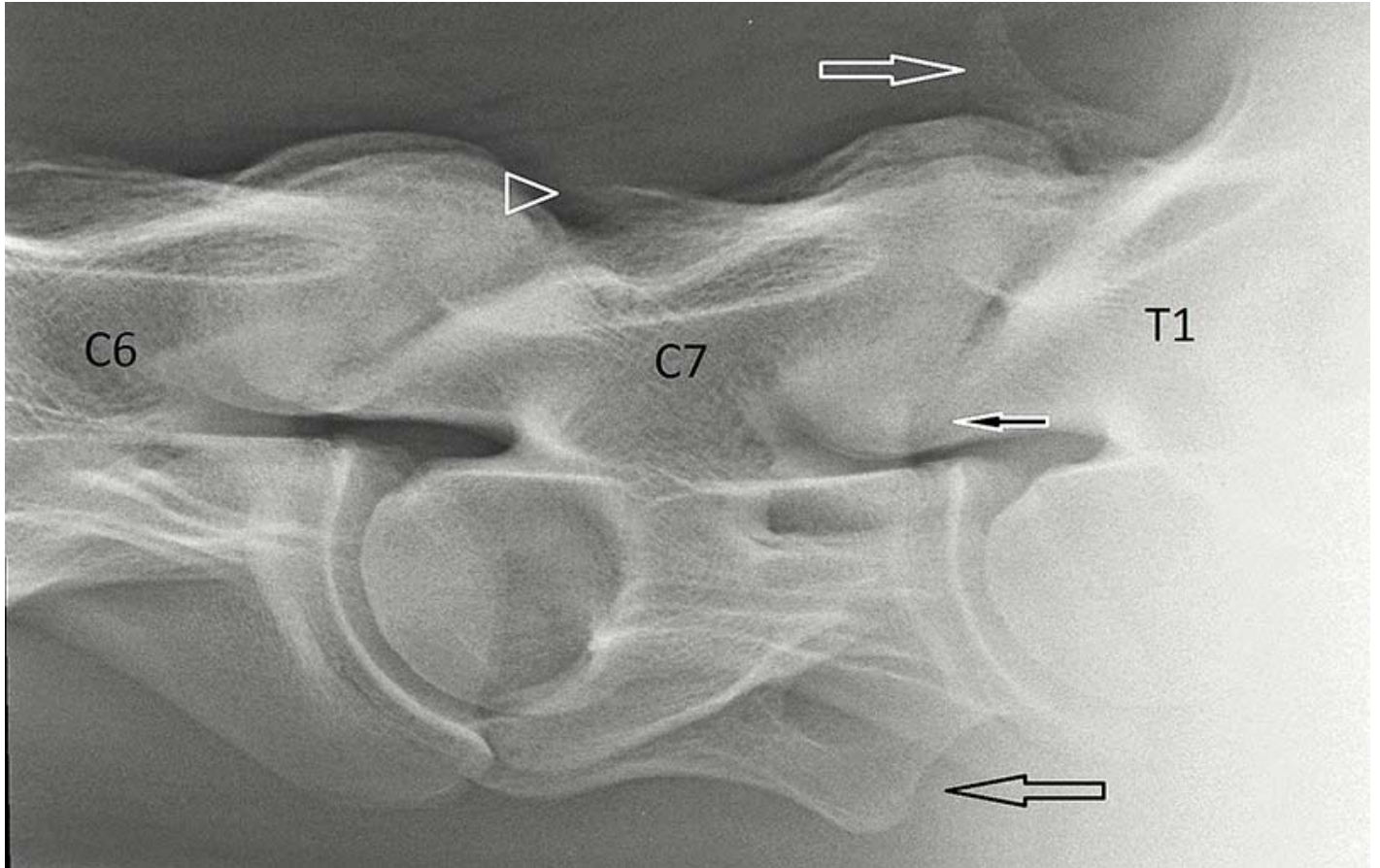


Figure 2. Lateral-lateral radiograph of the caudal aspect of the cervical spine and the 1st thoracic vertebra (T1). There is small spinous process on the 7th cervical vertebra (C7; arrowhead). The ventral processes of the 6th cervical vertebra (C6) are transposed to C7 (black arrow). The spinous process of T1 is short and squat. There is mild enlargement of the articular process joints between C7 and T1 (black and white arrow).

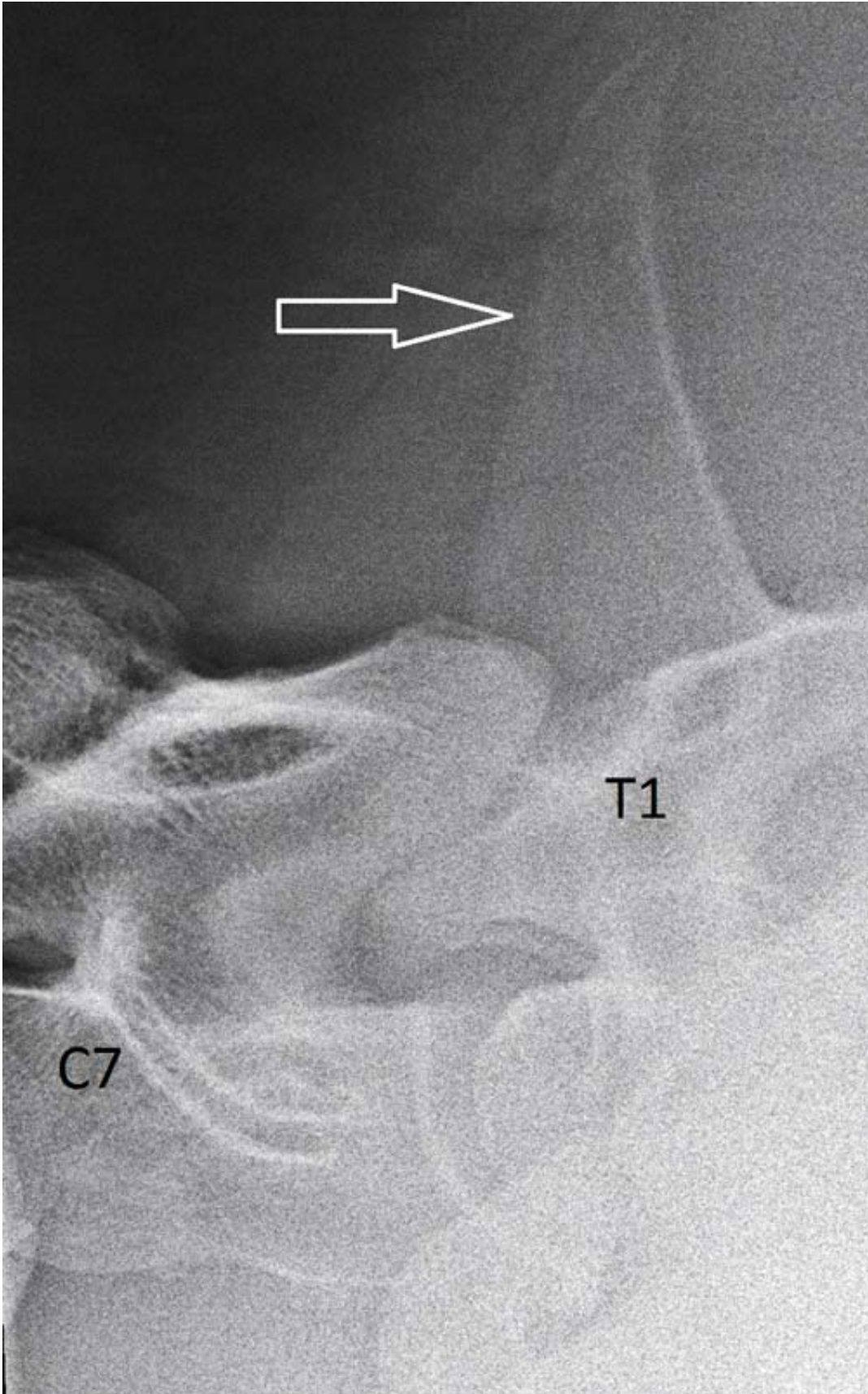


Figure 3. Lateral-lateral radiograph of the 7th cervical (C7) and 1st thoracic (T1) vertebra. The spinous process of T1 is high and pronounced (arrow).

The presence and shape of the spinous process was associated with breed – Thoroughbreds had the highest frequency of absence of the spinous process of the C7 vertebra and quarter horses had the highest frequency of a spur-shaped spinous process. Transposition of the ventral process from the C6 to the C7 was more common in females than in males. Short and squat spinous process of the T1 was associated with absence of the spinous process of the C7 and transposition of the ventral process.

DeRouen et al (2016) described the prevalence of anatomical variation of the C6 and associations with vertebral canal stenosis and articular process osteoarthritis in 100 mature horses that had undergone cervical radiography.

Cervical radiography had been performed for a number of reasons and included clinically normal horses and horses with cervical pain and/or neurological dysfunction. No standardised clinical and neurological examinations were applied to all horses. Morphological variations were found in 24%, symmetrical absence of the ventral process was recorded in 9% and asymmetrical absence in 15%. No gender predisposition was found, but Warmbloods were more likely to have an anomalous C6 than other breeds.

A significantly greater proportion of horses with an anomalous C6 had an intravertebral sagittal ratio of less than 0.5 at C6 (an intravertebral ratio of more than 0.5 was considered normal at C6). However, horses with an anomalous C6 were less likely to have neurological deficits attributable to the cervical region.

The authors pointed out the lack of accuracy of intravertebral sagittal ratio measurements for diagnosis of cervical vertebral stenotic myelopathy. No association was found between an anomalous C6 and osteoarthritis of the caudal articular process joints. A positive association existed between an anomalous C6 and perceived cervical pain or reduced range of motion. The authors speculated this association might be explained by alterations of the attachment sites for regional musculature, as described by May-Davis and Walker (2015), might lead to altered biomechanical forces.

A cadaver study documented transposition of the ventral process from the C6 to C7 in 33% of 78 horses (including 27 foals) that underwent postmortem CT examination of the cervical spine (Veraa et al, 2016). Transposition was seen unilaterally in 12 horses and bilaterally in 10. Associations between these morphological variations and vertebral canal diameter or abnormalities of the articular process joint were not assessed.

These articles highlight attention should be paid to the morphological variations of the caudal cervical vertebrae, because they might be associated with clinically significant abnormalities. Future studies are needed to confirm such associations and should be performed on a large population of horses undergoing standardised clinical examination, and should include clinically normal horses and horses with caudal cervical pain and/or neurological dysfunction.

Ideally, 3D imaging (CT) of the caudal cervical spine should also be performed to allow more accurate evaluation of anatomy, vertebral canal stenosis and abnormalities of the articular process joints.

Foot



Figure 4. Lateromedial radiograph of a foot. The palmar compact bone of the navicular bone is markedly thickened (arrow). In some horses, this can be associated with lesions in the deep digital flexor tendon (**Figure 5**). However, this may also represent a form of primary navicular bone pathology.

MRI is used to achieve accurate diagnosis in a considerable proportion of horses with foot pain when the results of radiography do not explain the lameness fully. However, in many cases, MRI is not available due to financial constraints or due to the lack of facilities and in these cases diagnosis is often made based on radiographic findings.

De Zani et al (2016) assessed the correlation of radiographic measurements of structures of the equine foot with lesions detected using MRI. Seventy-four feet of 52 horses with lameness localised to the foot underwent radiography and low-field magnetic resonance imaging. Objective

measurements were obtained on radiographs.

Although the authors stated horses had stood squarely and slightly oblique lateromedial radiographs had been excluded, not all images included for illustration were straight, which may have influenced measurements and, therefore, the results. Association between radiographic measurements and MRI findings were assessed.

Correlations existed between the thickness of the palmar compact bone of the navicular bone (**Figure 4**) and injuries of the deep digital flexor tendon (**Figure 5**), collateral sesamoidean ligament, navicular spongiosa and the proximal border of the navicular bone.

Long-toed horses had a high incidence of lesions involving the spongiosa and the proximal border of the navicular bone. Elongation of the navicular bone was associated with proximal and distal border injuries. A reduced palmar angle of the distal phalanx and increased angle between the middle and distal phalanges measured on the radiographs were seen in horses with abnormalities of the collateral ligaments of the distal interphalangeal joint and navicular bone spongiosa, respectively.

Recognition of such correlations might be useful to practitioners investigating foot pain without access to MRI. However, the relatively small number of horses and limitations of radiographic measurements in the study warrant interpretation of results with caution.

Fetlock

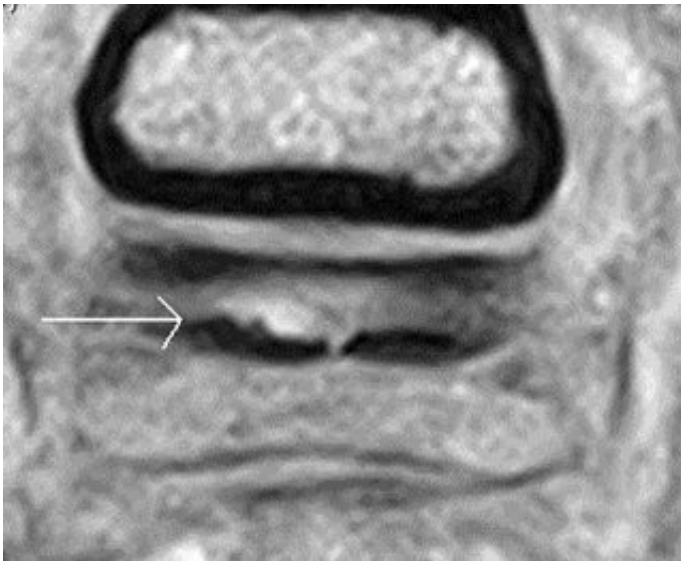


Figure 5. Transverse T1-weighted gradient echo low-field magnetic resonance images obtained at the level of the proximal aspect of the navicular bursa. A marked irregularity exists of the dorsal border of the deep digital flexor tendon (arrow), which was associated with soft tissue proliferation

in the navicular bursa.

MRI is used with increasing frequency as a part of investigation of lameness localised to the fetlock region. Cartilage lesions have been described on both low-field and high-field MRI images; however, the ability of low-field systems in particular to detect cartilage lesions without underlying subchondral bone abnormality has been questioned.

Porter et al (2016) assessed the correlation of articular cartilage thickness measurements acquired from magnetic resonance (MR), MR arthrography and CT arthrography images with gross articular cartilage thickness in the metacarpophalangeal joint. None of the imaging modalities correlated consistently with gross cartilage thickness. These results highlight the limitation of MRI to assess the articular cartilage, especially where curved articular surfaces are juxtaposed to each other as in the metacarpophalangeal and metatarsophalangeal joints (**Figure 6**).

Hock

Distal tarsal pain is common and radiographic examination is routinely performed as a part of lameness or pre-purchase examinations.

Skelly-Smith et al (2016) evaluated the centrodistal joint interosseous ligament region in 700 horses, including horses with and without pain causing lameness localised to the distal tarsal joints. The normal interosseous space was an oval or circular-shaped radiolucent area bordered proximally and distally by a rim of bone of uniform thickness and opacity.

Abnormalities in the interosseous ligament region of the lame(r) limb were identified in 121/700 (17.3% hocks and included loss of definition or complete loss of the oval-shaped radiolucent area, focal joint space narrowing adjacent to the interosseous space and mottled heterogeneous or increased opacity in the region of the interosseous ligament (**Figure 7**).

An association existed between abnormalities of the centrodistal joint interosseous ligament region and osteoarthritis of the centrodistal joint. However, these radiological abnormalities alone or in association with osteoarthritis were seen in both lame and non-lame limbs, indicating abnormalities in the interosseous ligament region can be asymptomatic.

Stifle

Lateral patellar ligament



Figure 6. Sagittal high-field T1-weighted gradient echo magnetic resonance image of a fetlock region. The articular cartilage appears as a uniform layer of intermediate signal intensity on the distal aspect of the third metatarsal bone (arrow). Note, it is impossible to differentiate between the articular cartilage of the third metatarsal bone and proximal phalanx where the articular surfaces are juxtaposed to each other.

Ultrasonography is routinely used for assessment of soft tissue injuries of the stifle. Detailed ultrasonographic appearance of normal and injured lateral patellar ligaments has only recently been described (Gottlieb et al, 2016).

Ultrasonographic examination of 12 horses without stifle-related lameness was performed and abnormalities were documented retrospectively in 18 horses with lateral patellar ligament injury. The normal lateral patellar ligament changed in appearance from the origin to its insertion. Proximally, it had ill-defined margins, then became flattened and bilobed over the lateral trochlear ridge. At the level of the femorotibial joint, the ligament was oval or triangular-shaped and had deeply irregular margins in the majority of stifles.

Irregular margins varied in appearance and ranged from single to multiple deep invaginations (by fat) that extended into the lateral patellar ligament body to a more subtle undulating appearance. Close to its tibial insertion the ligament was tapered, with striations.

The 18 horses with lateral patellar ligament injury represented 4% of all stifle examinations during the study period. Stifle wounds were present in 12 of the 18 horses. Most commonly, the mid and distal parts of the ligament were affected. Lateral patellar ligament injuries were severe in most

horses and associated with craniolateral stifle trauma, unlike middle patellar ligament injuries that often occur without a traumatic incident. Severe ultrasonographic abnormalities included enlargement, distortion of the normal architecture, and large hypoechoic to anechoic areas, with evidence of fibre tearing, with or without an osseous fragment.

A combination of radiography and ultrasonography was necessary to fully evaluate the extent of soft tissue and osseous lesions. The non-uniform appearance and the changing shape (from proximal to distal) of the lateral patellar ligament should be borne in mind when performing ultrasonographic examination of the stifle to avoid confusing these anatomical variations with lesions. Most injuries of the lateral patellar ligament are severe and associated with trauma.

Comparison of imaging modalities for diagnosis of intra-articular injuries



Figure 7. Dorsolateral-plantaromedial radiograph of a hock. An increased opacity exists in the region of the interosseous ligament of the centrodistal joint (arrow).

The value of three diagnostic imaging techniques and arthroscopy was compared for diagnosis of femorotibial joint disease in Western performance horses (Nelson et al, 2016). In this prospective study, 25 stifles of 24 horses underwent radiography, ultrasonography, CT arthrography and arthroscopy. Arthroscopy was more useful than other imaging modalities for detection of desmopathy of the cranial medial meniscotibial ligament, medial meniscal injury located on the craniolateral border and articular cartilage defects.

CT arthrography was able to detect desmopathy of the cranial medial meniscotibial ligament in

75% of arthroscopically observed cases and medial meniscal injury in 56% of arthroscopically detected cases. CT arthrography detected articular cartilage defects on the medial femoral condyle in 60% of cases; however, a significant disagreement existed between arthroscopy and CT arthrography.

Ultrasonography identified 27.3% of arthroscopically documented desmopathy of the cranial medial meniscotibial ligament and none of the craniolaterally located medial meniscal tears. CT arthrography detected more defects in the cruciate ligaments, proximal aspect of the tibia and ligament entheses than the other diagnostic imaging methods or arthroscopy, but was not reliable for detection of articular cartilage damage on the medial femoral condyle.

The authors concluded the information gained from CT or CT arthrography can lead to a more complete assessment of the stifle and this global understanding helped determine a more focused treatment and rehabilitation programme. They do not suggest CT arthrography has to be performed in all cases of stifle lameness, but should be considered in cases where the severity in clinical lameness cannot be explained by the findings on radiography or ultrasonography, to provide further information regarding bone or deep intra-articular soft tissues, or to obtain a more complete evaluation of structures in the femorotibial joints.

Several referral centres in the US use computed arthrography for diagnosing stifle injuries. Most CT units available in the UK do not allow examination of the stifle in live adult horses. A system with a large bore gantry has become available, but to the authors' knowledge improvements are required before it can be used for examination of the stifle. However, as suggested previously, 3D imaging (CT or MRI) would certainly enhance diagnostic capabilities for stifle injuries and it should be aimed for.

This review demonstrates sophisticated diagnostic imaging methods, such as MRI or CT, not only provide previously inaccessible information, but can also improve our interpretation of conventional diagnostic imaging results. We also continue learning about the presence and significance of anatomical variations, many of which can be detected by radiography and/or ultrasonography.

References

- DeRouen A, Spriet M and Aleman M (2016). Prevalence of anatomical variation of the sixth cervical vertebra and association with vertebral canal stenosis and articular process osteoarthritis in the horse, *Veterinary Radiology and Ultrasound* **57**(3): 253-257.
- De Zani D, Polidori C, di Giancamillo MD and Zani DD (2016). Correlation of radiographic measurements of structures of the equine foot with lesions detected on magnetic resonance imaging, *Equine Veterinary Journal* **48**(2): 165-171.
- Gottlieb R, Whitcomb MB, Vaughan B, Galuppo LD and Spriet M (2016). Ultrasonographic appearance of normal and injured lateral patellar ligaments in the equine stifle, *Equine Veterinary Journal* **48**(3): 299-306.

- May-Davis S (2014). The occurrence of a congenital malformation in the sixth and seventh cervical vertebrae predominantly observed in thoroughbred horses, *Journal of Equine Veterinary Science* **34**(11-12): 1,313-1,317.
- May-Davis S and Walker C (2015). Variations and implications of the gross morphology in the longus colli muscle in Thoroughbred and Thoroughbred derivative horses presenting with a congenital malformation of the sixth and seventh cervical vertebrae, *Journal of Equine Veterinary Science* **35**(7): 560-568.
- Nelson B, Kawcak CE, Goodrich LR, Werpy NM, Valdes-Martinez A and McIlwraith CW (2016). Comparison between computed tomographic arthrography, radiography, ultrasonography, and arthroscopy for the diagnosis of femorotibial joint disease in Western performance horses, *Veterinary Radiology and Ultrasound* **57**(4): 387-402.
- Porter EG, Winter MD, Sheppard BJ, Berry CR and Hernandez JA (2016). Correlation of articular cartilage thickness measurements made with magnetic resonance imaging, magnetic resonance arthrography, and computed tomographic arthrography with gross articular cartilage thickness in the equine metacarpophalangeal joint, *Veterinary Radiology and Ultrasound* **57**(5): 515-525.
- Santinelli I, Beccati F, Arcelli R and Pepe M (2016). Anatomical variation of the spinous and transverse processes in the caudal cervical vertebrae and the first thoracic vertebra in horses, *Equine Veterinary Journal* **48**(1): 45-49.
- Skelly-Smith E, Ireland J and Dyson S (2016). The centrodistal joint interosseous ligament region in the tarsus of the horse: normal appearance, abnormalities and possible association with other tarsal lesions, including osteoarthritis, *Equine Veterinary Journal* **48**(4): 457-465.
- Veraa S, Bergmann W, van den Belt A-J, Wijnberg I and Back W (2016). Ex vivo computed tomographic evaluation of morphology variations in equine cervical vertebrae, *Veterinary Radiology and Ultrasound* **57**(5): 482-488.